JOURNAL OF THE ROYAL SOCIETY Interface

rsif.royalsocietypublishing.org

Research

Cite this article: Huang D, Niu L, Wei Y, Guo M, Zuo Y, Zou Q, Hu Y, Chen W, Li Y. 2014 Interfacial and biological properties of the gradient coating on polyamide substrate for bone substitute. *J. R. Soc. Interface* **11**: 20140101.
http://dx.doi.org/10.1098/rsif.2014.0101

Received: 29 January 2014
Accepted: 28 February 2014

Subject Areas:
biomedical engineering, biomaterials

Keywords:
interfacial properties, gradient coating, polyamide, nano-hydroxyapatite, osteogenesis

Authors for correspondence:
Di Huang
e-mail: huangdi@tyut.edu.cn
Yi Zuo
e-mail: zoae@vip.sina.com
Yubao Li
e-mail: nic7504@scu.edu.cn

Electronic supplementary material is available at http://dx.doi.org/10.1098/rsif.2014.0101 or via http://rsif.royalsocietypublishing.org.

Royal Society Publishing

Interfacial and biological properties of the gradient coating on polyamide substrate for bone substitute

Di Huang[1,2], Lulu Niu[1], Yan Wei[1], Meiqing Guo[1], Yi Zuo[2], Qin Zou[2], Yinchun Hu[1], Weiyi Chen[1] and Yubao Li[2]

[1]Department of Biomedical Engineering, Shanxi Key Laboratory of Material Strength and Structural Impact, College of Mechanics, Taiyuan University of Technology, Taiyuan 030024, People's Republic of China
[2]Research Center for Nano-Biomaterials, Analytical and Testing Center, Sichuan University, Chengdu 610064, People's Republic of China

Fabrication of bioactive and mechanical matched bone substitutes is crucial for clinical application in bone defects repair. In this study, nano-hydroxyapatite/polyamide (nHA/PA) composite was coated on injection-moulded PA by a chemical corrosion and phase-inversion technique. The shear strength, gradient composition and pore structure of the bioactive coating were characterized. Osteoblast-like MG63 cells were cultured on pure PA and composite-coated PA samples. The cells' adhesion, spread and proliferation were determined using MTT assay and microscopy. The results confirm that the samples with the nHA/PA composite coating have better cytocompatibility and have no negative effects on cells. To investigate the *in vivo* biocompatibility, both pure PA and composite-coated PA cylinders were implanted in the trochlea of rabbit femurs and studied histologically, and the bonding ability with bone were determined using push-out tests. The results show that composite-coated implants exhibit better biocompatibility and the shear strength of the composite-coated implants with host bone at 12 weeks can reach 3.49 ± 0.42 MPa, which is significantly higher than that of pure PA implants. These results indicate that composite-coated PA implants have excellent biocompatibility and bonding abilities with host bone and they have the potential to be applied in repair of bone defects.

1. Introduction

Metallic materials are most commonly used for load-bearing implants and internal fixation devices owing to the high ductility, high yield strength and corrosion resistance [1–3]. However, a material with high elastic modulus may not be ideal for load-bearing implants. This is because insufficient load transfer from an artificial implant to the adjacent remodelling bone may result in bone resorption and eventual loosening of the prosthetic device [4,5]. Differently from metallic materials, polymeric materials, such as polyetheretherketone, polytetrafluoroethylene, polyuransine and polyamide (PA), can overcome these problems owing to certain advantages, such as facile processabilities, excellent mechanical properties and regulative and controllable features [6–9]. Therefore, polymeric materials are excellent candidates for use in permanent bone repair.

As we know, the long-term performance of load-bearing bone-replacement material depends not only on the bioactivity of the materials, but also on stable mechanical properties. Appropriate biomechanical strength, inability to be absorbed and degraded, ease of processing, lack of toxicity and sterilization resistance made PA the ideal candidate for permanent bone replacement [10,11]. However, PA lacks bioactivity with natural bone and cannot provide Ca and P elements for bone reconstruction. Thus, the application of neat PA in bone repair is limited. Generally, the interaction between polymers and cells/tissues at the tissue–implant interface is strongly related to the surface composition and structure. Therefore, surface engineering of polymers is an interesting way

to modify the material and biological responses [12]. There have been several ways to improve the bioactivity of PA for bone repair, such as compounding with bioactive inorganic particles [8,13], grafting with bioactive groups [14] and forming bioactive coatings [5,15]. Compared with the first two methods, bioactive coating is a relatively facile and low-cost technique.

Nano-hydroxyapatite (nHA), owing to its chemical similarity to the inorganic component of natural bone, has been widely used for bioactive coating of orthopaedic implants [12,13,16–18]. To improve the integration ability of the implants with the nearby bone tissues, a number of different coating techniques have been employed for the preparation of nHA-coated implants, which includes solution-based techniques [4,19,20], ionic sputtering [21,22] and plasma spraying [23,24]. Ionic sputtered and thermally sprayed nHA coatings are already used successfully for metallic implants, but coating techniques have not yet been developed for polymer composites due to quite challenging heat management and adhesion concerns.

To fabricate nHA or nHA composite coating on a PA matrix, solution-based techniques have been developed. It has been reported that bioactive apatite is deposited on a PA matrix containing carboxyl groups or sulfonic groups by biomimetic processes [4,5,25]. However, the apatite layer formed is very thin and easy to peel off from the matrix. Polymer/nHA composite coating is also fabricated for its antibacterial property or excellent cell response, but the composite coating suffers from poor interfacial bonding and a sharp coating–substrate interface, which can reduce the adhesion strength between the substrate and the composite coating [26,27]. Therefore, it is important to develop a structurally stable coating with a composition gradient across the coating thickness [28].

In a previous study, our research group developed a novel nHA/PA composite for bone repair and reconstruction using a co-precipitation method. We have already demonstrated that nHA/PA composite possesses superior biocompatibility, osteogenesis and strong bonding between HA nanocrystals and PA matrix [13,29]. Based on the same polymer component, nHA/PA composite coating fabricated on PA laminae exhibited a gradient nHA composition and porous structure. The porous coating integrated seamlessly with the dense PA substrate via a porous chemical corrosion region extending from the PA matrix, which produced potential high interfacial bonding strength. The advantage of such a combination is obvious. The porous chemical corrosion region acts as a diffuse and strong interface between the substrate and the composite coating, forming a compositionally and structurally graded coating, which can eliminate problems associated with sharp interfaces. The present work focuses on processing, coating characterization, *in vitro* and *in vivo* biocompatibility and the bonding ability with bone of the compositionally graded HA coatings on PA prepared using a chemical corrosion and phase-inversion technique.

2. Material and methods

2.1. Materials preparation

2.1.1. Fabrication of nano-hydroxyapatite/polyamide composite slurry

Polyamide66 (PA) with a viscosity-average molecular weight of 1.8×10^4 was purchased from Asahi Chemical Industry Co. Ltd, Japan. The nHA and PA composite slurry was prepared using the co-precipitation method in ethanol [8,11]. Briefly, PA granules were completely dissolved into ethanol solution at 70°C for 3 h. The nHA crystals slurry, prepared using wet synthesis [30], was dispersed by anhydrous ethanol and then gradually added into PA ethanol solution with vigorous stirring at 70°C for another 3 h. The weight ratio of nHA crystals to PA was 50 : 50. When a homogeneous system was obtained, the mixture was kept in a sealed container at room temperature.

2.1.2. Fabrication of polyamide substrate

The pelletized PA was dried at 100°C for 12 h in a vacuum chamber and moulded into cylindrical specimens of 2.5 mm in diameter and 6 mm in length and laminae of 1 mm in thickness by injection moulding (KTC-200, Kinki, China). The injection temperature ranged from 240°C to 270°C under 30 MPa pressure. Then, the as-prepared specimens were cleaned ultrasonically in distilled water and dried at 60°C for 6 h.

2.1.3. Nano-hydroxyapatite/polyamide composite coating on polyamide substrate.

The PA specimens were immersed in nHA/PA composite slurry with a viscosity of 5000 mPa s with gentle stirring at 37°C for 4 h. Then the samples were removed from the composite slurry and dried in air at 60°C for 24 h, during which the phase change of ethanol from liquid to gas caused the formation of an interconnected porous coating. Finally, the obtained samples were cleaned ultrasonically in distilled water to fully eliminate the residual ethanol and air-dried at room temperature.

2.2. Characterization

2.2.1. Scanning electron microscopy and energy-dispersive X-ray spectroscopy

The composite-coated cylindrical samples were fractured in liquid nitrogen and the fracture surface was observed using scanning electron microscopy (SEM, JSM-6500LV, Japan). Energy-dispersive X-ray spectroscopy (EDS, Oxford, UK) on the SEM was used to analyse the elements. Prior to examination, each sample was coated with gold.

2.2.2. Interfacial bonding strength

The lamina specimens were cut into a rectangle shape of $10 \times 40\ mm^2$ for the interfacial bonding strength between the coating and substrate. According to ASTM-F1044, the bonding strength was conducted on a universal mechanical testing system (AGIC 50KN, Shimadzu, Japan) with a crosshead moving rate of $0.5\ mm\ min^{-1}$ [31]. As the schematic shown in the electronic supplementary material, figure S1, two composite-coated lamina specimens were adhered together by epoxy resin (Epoxy Adhesives DG-3S, Chengrand, China). The value of the shear strength was calculated from the fractured force over the stressed area. Three specimens were tested in each group. After testing, the fracture surface of the specimens was analysed by SEM and EDS.

2.3. Cytocompatibility *in vitro*

Human osteosarcoma cell lines (MG63) were employed to evaluate the cytocompatibility of the PA substrate and nHA/PA-coated samples. The MG63 cells were routinely cultured in F12 medium (Cell-culture grade, Biowhittaker, Walkersville, MD, USA) supplemented with 10% volume fraction of calf serum (cell-culture grade, Gibco, Rockville, MD, USA), 1% L-glutamine and 1% penicillin/streptomycin. Cells were sub-cultured every 3 days in a humidified incubator with 95% air and 5% CO_2 at 37°C and the medium was changed every 2 days.

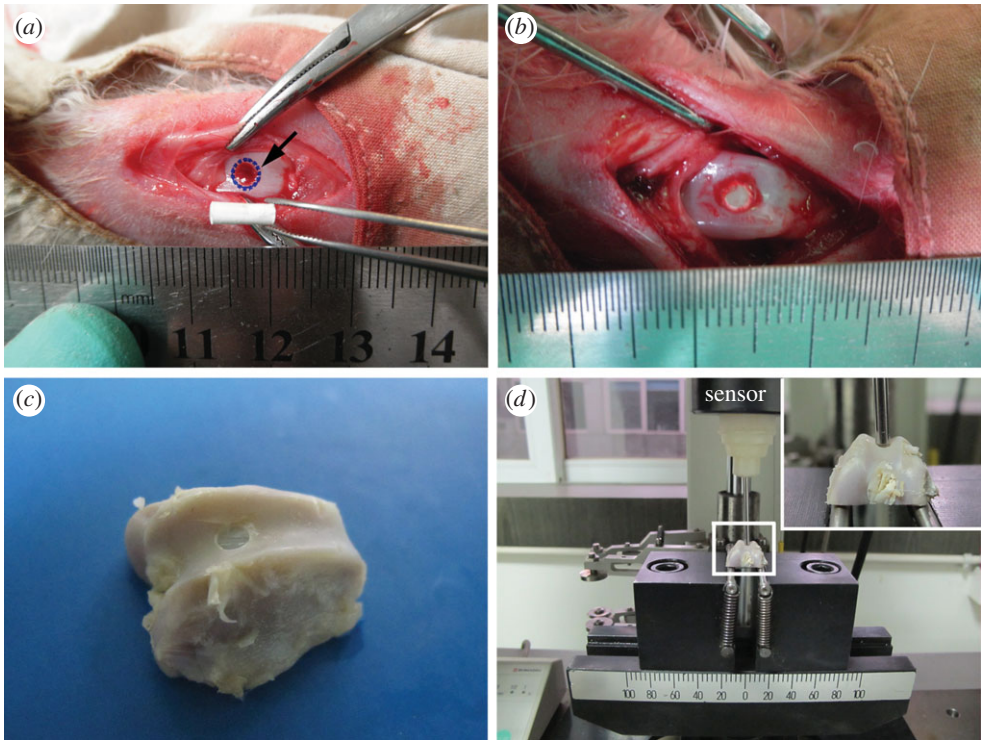

Figure 1. Surgery process and push-out test. (*a*) A hole of 3 mm in diameter and 6 mm in depth was drilled into the trochlea of rabbit femurs, as indicated by the arrow. (*b*) A sample was implanted in the hole. (*c*) The sample was harvested at periods and cut into the shape (the cylindrical implants was exposed and perpendicular with the horizontal bottom of samples). (*d*) The sample was placed on a support jig mounted on the universal mechanical testing machine. The stems in the surrounding tissues were pushed out with a metal rod (2.5 mm in diameter). (Online version in colour.)

The lamina samples with and without nHA/PA composite coating were cut into discs with a diameter of 10 mm and height of 1 mm and disinfected by ethylene oxide gas for 3 h. The sterilized samples were put into 24-well plates and incubated in 1 ml MG63 cells suspension (about 2×10^4 cells per well). Afterwards, the seeded specimens were cultured in a humidified incubator (37°C, 5% CO_2) for 4 days. The cells were visualized using a phase-contrast microscope (Nikon TE300, Melville, Japan). For visualization of the growth and distribution of MG63 cells on the surface of each specimen, MG63 cells were pre-labelled with fluorescent 3,3′-dioctadecyloxacarbocyanine perchlorate (DiO) dye (Molecular Probes, China) at 37°C for 20 min following the manufacture's protocol. The labelled cells were then seeded on samples as previously described [15]. The cells grown on the discs were then observed using a fluorescence microscope (Nikon TE300, Melville, Japan) at day 4 after seeding.

The proliferation of MG63 cells with samples or control was determined using an MTT (3-{4,5-dimethylthiazol-2y}-2,5-diphenyl-2H-tetrazolium-bromide) assay. Briefly, at each experimental interval (at day 1, 3, 5 and 7), the medium was discarded, then 40 µl MTT solution was added into each well. After incubation for 4 h at 37°C, the MTT solution was removed and the precipitated formazan was dissolved in DMSO (150 µl/well). The absorbance of solubilized formation at 570 nm was recorded with a microplate spectrophotometer (Perkin Elmer Co. Ltd, USA). All of the experiments were performed in triplicate.

2.4. Biocompatibility and bone bonding *in vivo*

2.4.1. Surgery implantation and histology

Thirty healthy New Zealand white rabbits weighting about 2.5 kg each were selected for the animal study. The animals were anaesthetized with pentobarbital sodium (0.1 mg kg^{-1} of body weight). Surgery was performed under sterile condition. Each femoral knee metaphysic was exposed by a skin incision and a patella flap. A defect deep to subchondral bone was created using dental drill (Escort III, Korea) at the trochlea of the femur to obtain cylindrical defects with 3 mm in diameter and 6 mm in depth (figure 1*a*). Groups consisted of the pure PA implant group and the nHA/PA composite-coated PA implant group. After anaesthetization, the PA samples and composite-coated PA constructs were implanted in the defect sites in each group (figure 1*b*). The wounds were closed with sterile suture, and the animals were returned to a housing facility, where they had free access to food and water. After four and 12 weeks, the rabbits were sacrificed and femoral condyles were collected.

2.4.2. Push-out testing

The samples harvested at four and 12 weeks were cut into the shape as shown in figure 1*c*. A flat bottom surface was obtained using a high-speed, water-cooled sawing machine (SHERLINE-5410, USA), with the cylindrical implants exposed and perpendicular with the flat bottom surface of the samples to make the push-out test possible [32]. Subsequently, the sample was placed on a support jig mounted on the universal mechanical testing system (AGIC 50 KN, Shimadzu, Japan). This support jig enabled the application of a vertical force using a 2.5 mm diameter metal rod (at a constant displacement speed of 0.5 mm min^{-1}) on the cylindrical implants (as shown in figure 1*d*). The mechanical strength of the defects filled with implants was calculated according to shear strength (MPa) $= F/(\pi \times D \times H)$, where F is the push-out force (N), D and H are the diameter and height of the implants, respectively. Each value represents an average of three runs.

2.4.3. Scanning electron microscopy and energy-dispersive X-ray spectroscopy

At the time of sacrifice (12 weeks), the femoral condyles containing the cylindrical implants were cut into two sections axial normal to the long axis of the implants using the high-speed, water-cooled sawing machine. Then the specimens were fixed

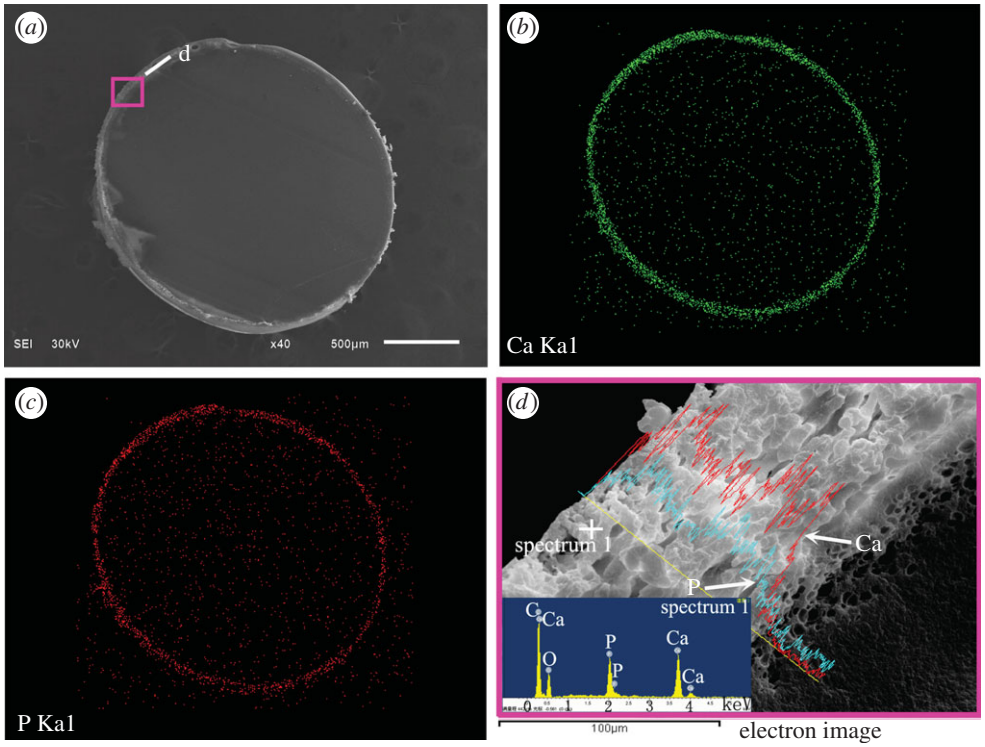

Figure 2. (*a*) The morphology of the cross section of nHA/PA composite-coated implant; (*b*) map scanning of Ca element and (*c*) P element, respectively; line-scanning of Ca and P element corresponding to the rectangle in (*a*) and the inset is the EDS spectra reflected the spectrum 1 (*d*). (Online version in colour.)

with 3% volume fraction of glutaraldehyde for 2 days, dehydrated in ethanol solutions with concentrations of 50, 70, 80, 90 and 100% for 3 days in each solution, rinsed with isoamyl acetate, dried with supercritical CO_2 and observed with SEM. EDS chemical analyses were performed to investigate the interface between the implants and cancellous bone.

2.4.4. Histological evaluation

The femoral condyles containing the cylindrical implants were excised at the time of sacrifice (four and 12 weeks). The collected samples were fixed and stored in 10% neutral-buffered formalin and decalcified in 10% EDTA. Standard dehydration in sequentially increasing ethanol solutions to 100% ethanol was performed followed by immersion in xylene, paraffin-saturated xylene and finally molten paraffin. Longitudinal sections of 5 μm in thickness were prepared through the centre of the cylindrical implantations. The sections were stained by Masson using orange G, phosphotungstic acid and methyl blue and observed using a light microscope.

2.5. Statistical analysis

The data were collected in ORIGIN 8.0 software and the results were expressed as means and standard deviations. Statistical significance was determined using SPSS (v. 10.0) software. Two experimental groups were evaluated by Student's *t*-test. A value of $p < 0.05$ was considered statistically significant.

3. Results

The cross-section surface of a nHA/PA-coated cylindrical implant is shown in figure 2. The map scanning of Ca and P elements determined by EDS shows that nHA is the main component of the coating surface. The cross-section microstructure in figure 2*d* shows the dense substrate, corroded layer (approx. 25 μm thick), and nHA-rich coating layer (approx. 90 μm thick) and the EDS element analysis. It can be seen that the pore size increases slightly from the substrate to the coating layer. The composition of the coating layer is determined by the EDS, and the inset EDS spectra show the existence of C, Ca and P in the area nearby the surface. No evidence of other impurities has been found in the EDS data. Moreover, the Ca/P content is increasing from the interface between the porous corroded layer and porous coating layer to porous coating surface. The porous corroded layer without Ca/P demonstrates that PA is the chief component of the corroded layer.

The interfacial shear strength of the nHA/PA coating and PA substrate prepared at 37°C for 4 h is 4.58 ± 0.14 MPa. After the bonding test, the fracture surface of the samples is shown in figure 3. From the fracture morphology, the pores deform along the direction of the external load (as the arrows shown in figure 3*b*). The corresponding EDS C and Ca-map scanning shows the main component of the fracture surface is C element and no Ca element can be observed. It demonstrates that the fracture occurs inside the corroded layer.

Figure 4 shows representative phase-contrast micrographs of MG63 cells cultured on pure PA and nHA/PA-coated samples for 1 day and 4 days. At 1 day, only a few cells can be seen around the semi-transparent injection-moulded PA laminae. Many more cells with an elongated fusiform shape spread around opaque nHA/PA-coated samples. At 4 days, a large amount of cells proliferate around both samples. The samples with or without nHA/PA coating have no negative effects on MG63 cells.

To further understand the cells growth and proliferation on the surface of the pure PA and nHA/PA-coated samples, the MG63 cells were visualized by DiO labelling at 4 days after seeding. As shown in figure 5, the cells spread well on both samples and exhibit a similar spindle-like appearance. However, the cell population attached to nHA/PA-coated

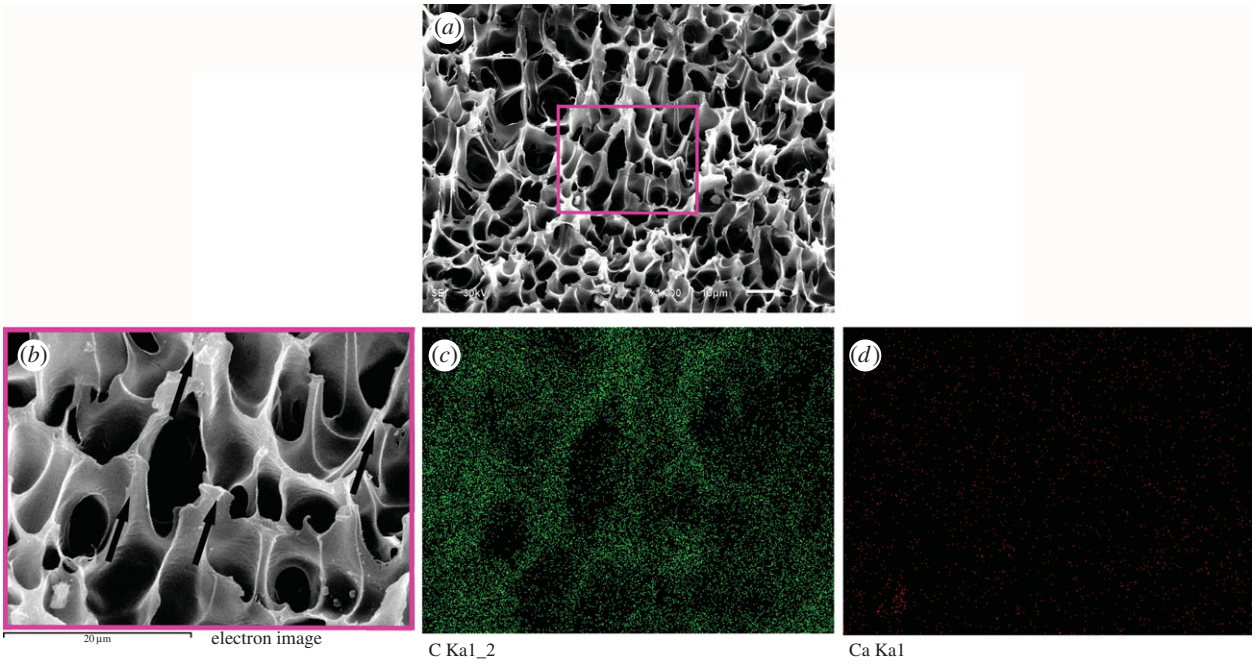

Figure 3. SEM photographs and EDS map-scanning analysis of the fracture surface after bonding test: fracture surface of the sample (*a*); higher magnification corresponding to the rectangle in (*a*), and the arrows denote the direction of shear force; map-scanning analysis of C element (*c*) and Ca element (*d*) corresponding to (*b*). (Online version in colour.)

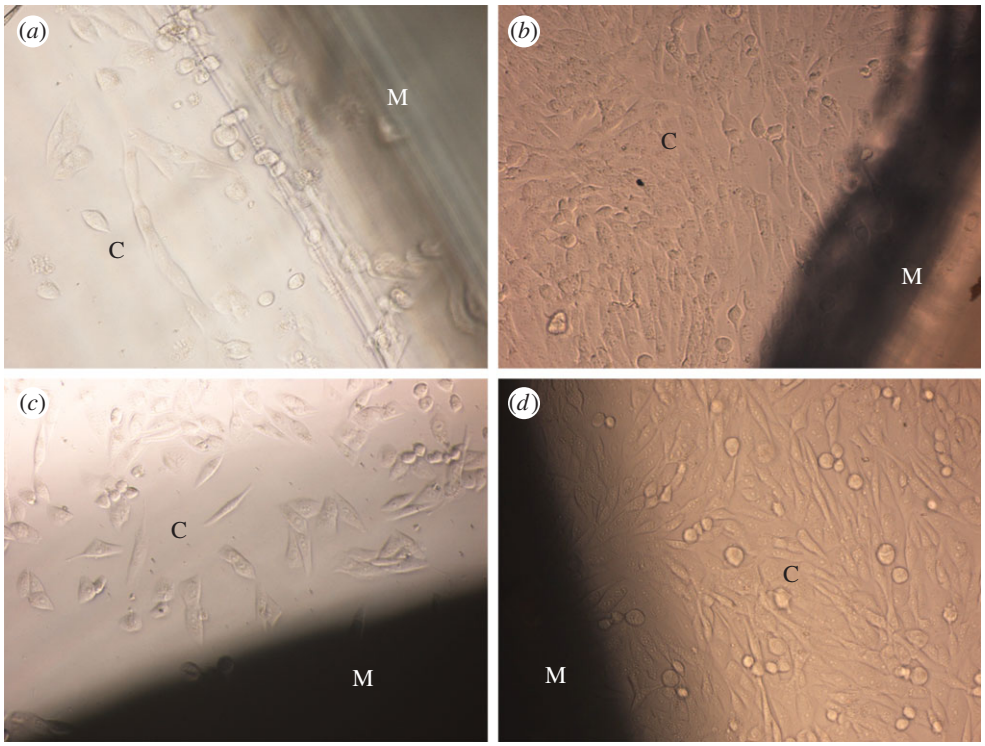

Figure 4. Phase-contrast micrographs of MG63 cells (denoted as C) cultured on PA laminae before and after nHA/PA composite coating: MG63 cells cultured on native PA laminae (denoted as M) for (*a*) 1 day and (*b*) 4 days; MG63 cells cultured on nHA/PA composite-coated PA laminae (denoted as M) for (*c*) 1 day and (*d*) 4 days. (Online version in colour.)

samples is higher than that of pure PA laminae. The result proves that the composite-coated samples have excellent cytocompatibility.

After 1, 3, 5 and 7 day(s) of culturing, the cell proliferation in each group was assessed using the MTT test. As represented in figure 6, during a period of 7 days of culture, the cells proliferate tremendously with the culture time in all groups. At the early stage (days 1 and 3), there is no significant difference between both experimental groups. After 5 days co-culturing, the proliferation of cells cultured on nHA/PA composite-coated samples shows a significant difference from the pure PA group ($p < 0.01$) and the control group ($p < 0.05$). At day 7, the cell proliferation cultured on composite-coated samples increases significantly compared with PA substrate ($p < 0.05$) and control group ($p < 0.001$). The results demonstrate that the nHA/PA composite-coated samples have better cytocompatibility.

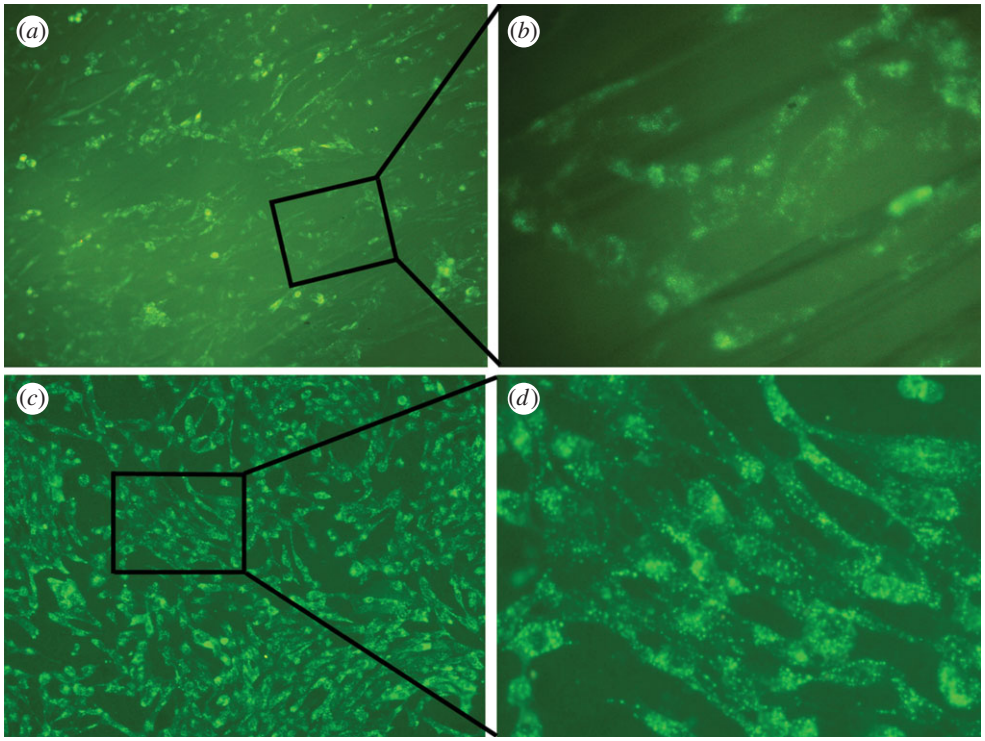

Figure 5. Fluorescent micrographs of DiO-labelled MG63 cells cultured for 4 days on: (*a*) PA laminae and (*b*) higher magnification of MG63 cells corresponding to the rectangle in (*a*); (*c*) nHA/PA composite-coated PA laminae and (*d*) higher magnification of cells corresponding to the rectangle in (*c*). (Online version in colour.)

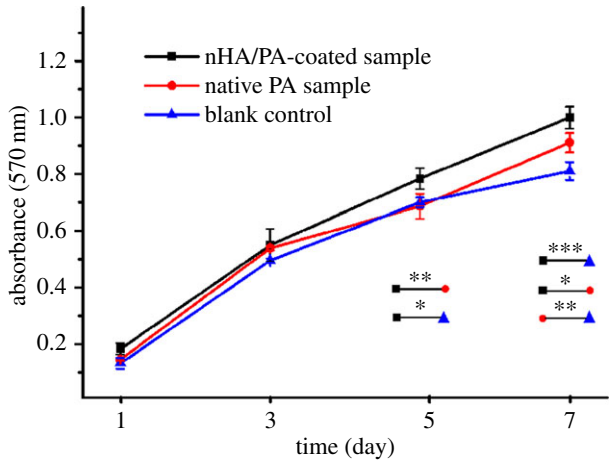

Figure 6. MTT assay for proliferation of MG63 cells cultured on PA laminae and nHA/PA composite-coated samples for 1, 3, 5 and 7 day(s), compared with the blank control (tissue culture plastic) under the same culture conditions. Significantly different at $*p < 0.05$, $**p < 0.01$ and $***p < 0.001$. (Online version in colour.)

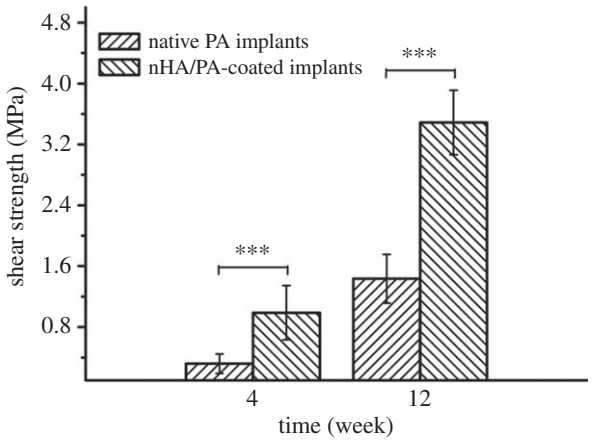

Figure 7. Push-out test results of native PA cylindrical samples and nHA/PA composite-coated samples after four and 12 weeks of implantation. Significantly different at $***p < 0.001$.

The results of the push-out test show a gradual increase in mechanical strength with increasing implantation periods. After four weeks of implantation, the push-out value of the pure PA implants was 0.32 ± 0.13 MPa, which increased to 0.99 ± 0.35 MPa at 12 weeks. The nHA/PA composite-coated PA implants show a mechanical strength value of 1.44 ± 0.32 MPa after four weeks of implantation, which increased to 3.49 ± 0.42 MPa after 12 weeks of implantation. At individual implantation periods, nHA/PA composite-coated samples show a significant difference with pure PA implants ($p < 0.001$) (figure 7).

After harvesting at 12 weeks, the interfaces between the bone and the implants are shown in figure 8. Results suggest an intimate contact between the bone and both the PA implant surface and the nHA/PA composite-coated PA implant surface. EDS analyses show that the Ca/P content decreases sharply from the bone regions to the PA implant. However, Ca/P content decreases gradually from bone tissue to composite-coated implant. The nHA/PA coating layer served as a continuous link between the bone tissue and the dense PA implant.

Figure 9 shows the optical microstructure of the interfaces between the implants and new bone stained by Masson after four and 12 weeks post-implantation. For the naked PA implants, a clear interval between PA implant and bone tissue was observed after four weeks post-implantation. After 12

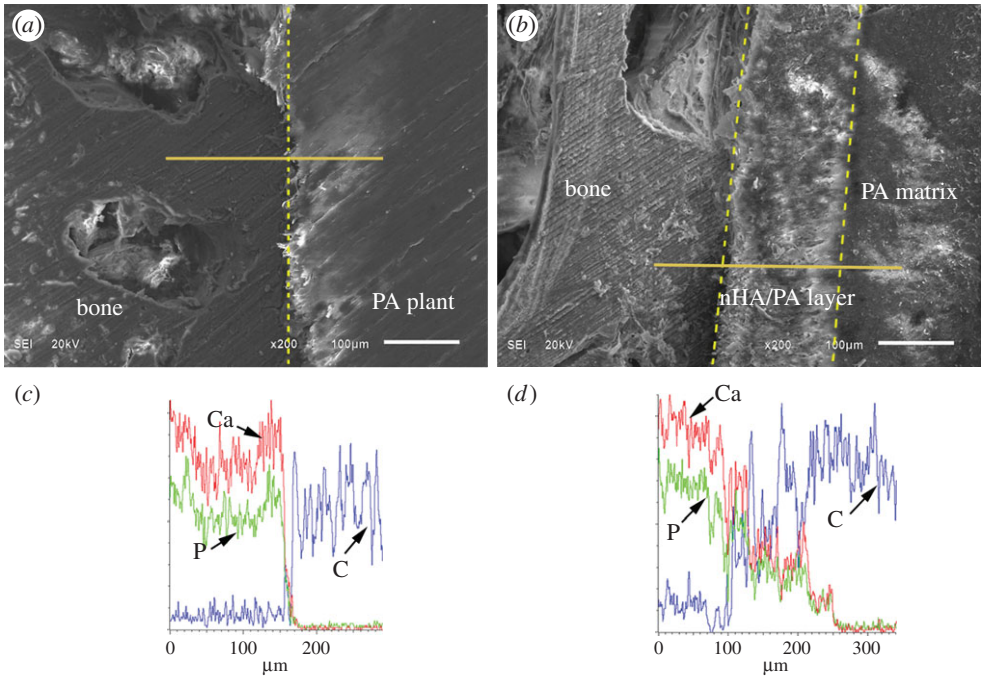

Figure 8. SEM images and line-scan EDS in an area including cancellous bone, implant and their interface: interface (dotted line in (*a*)) between cancellous bone and PA implant (*a*) and corresponding EDS analysis (*c*); interface between cancellous bone and nHA/PA composite-coated PA implant (*b*) and corresponding EDS analysis (*d*). (Online version in colour.)

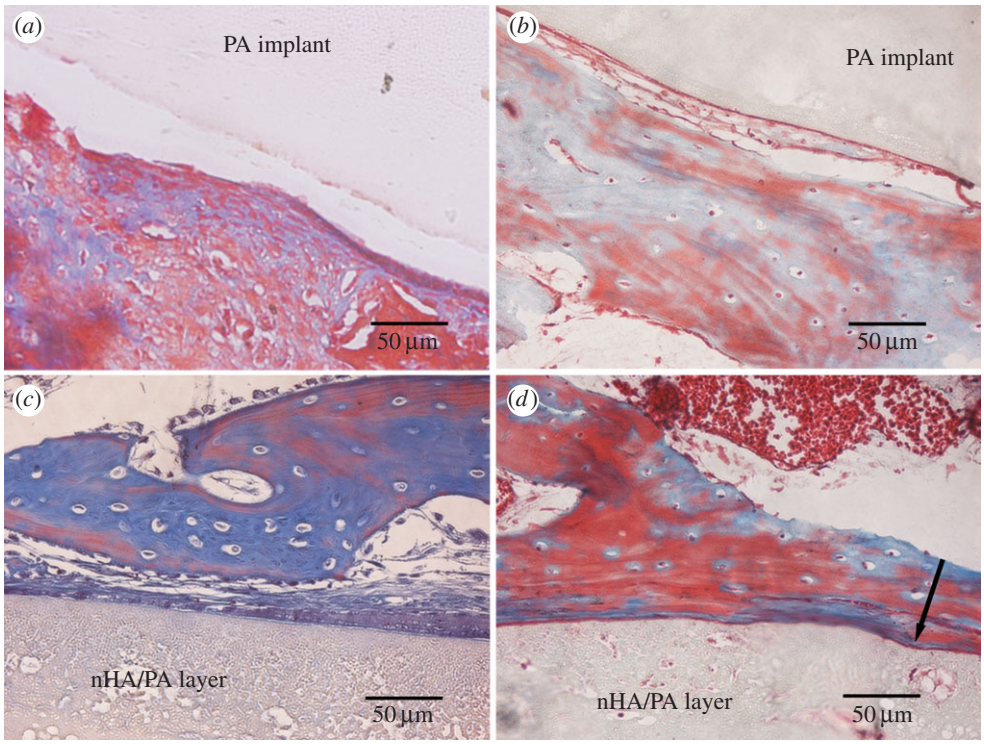

Figure 9. Masson-stained sections of pure PA implantations (*a*,*b*) and nHA/PA composite-coated implantations (*c*,*d*), which were harvested at four (*a*,*c*), and 12 (*b*,*d*) weeks post-implantation. The arrow in (*d*) denotes the deformation of the composite coating due to the load from the surrounding new bone. (Online version in colour.)

weeks implantation, newly formed osteoid tissue attaches to PA surface and it seems a relatively tight contact between the implant and the bone as indicated in figure 9*b*. For the nHA/PA-coated implants, connective tissue was seen at the interface after four weeks post-implantation. At week 12, the connective tissue became thinner and was replaced by osteoblasts and bone matrix. Newly formed osteoid tissue and newborn bone trabeculae almost covered the implant surface completely. The deformation of the nHA/PA coating layer is observed due to the load from the surrounding new bone (indicated by the arrow).

4. Discussion

At the present time, the aim of bone repair material is to provide the requisite durability, functionality and biological response. Durability and functionality are governed by the bulk properties of the material, whereas biological response

depends on the surface properties [22,33,34]. Therefore, it is very important to optimize mechanical properties of bone repair materials and construct the bioactive surface to be integrated into bone tissues. In this study, we chose non-degradable PA as the substrate because of its mechanical strength and modulus similar to natural cortical bone. It effectively avoids stress screen and provides stable mechanical performance [13,15]. To enhance the surface bioactivity of the PA substrate, it is crucial to create two interfaces. One is the interface between the coating and the substrate, the other is the interface between the coating and the bone tissues. For the former interface, the nHA/PA composite was coated onto the PA substrate by a chemical corrosion and phase-inversion technique. From the cross section of the PA cylinder, the transition of interface between the matrix and coating layer seems quite natural via the common PA component. As discussed earlier, the composite coating shows a gradient variation in both microstructure and chemical composition. Coating with such a gradient structure is usually believed to be excellent in clinical application [28,35].

One important factor when considering the desirable properties of an implant coating is that the coating should be strongly bonded to the implant to maintain implant integrity [2]. Therefore, the shear strength between the coating and substrate becomes one of the most important mechanical properties for coated implants that would affect the ultimate success in clinical application. In the previous study, few reports provided the bonding strength between apatite and polymer matrix. Fewer reports improve the adhesion strength by pre-treatment of polymer matrix. After pre-treatment, the adhesive strength of the formed apatite layer to the polymethylmethacrylate (PMMA) and PA6 were increased from 1.1 to 2.8 MPa and from 0.6 to 3.1 MPa, respectively [36]. However, the bonding strength between apatite and polymer substrate is still lower than that reaction at 37°C in our study (4.58 ± 0.14 MPa). In our previous study, we demonstrated that the bonding strength is relative to the reaction conditions (reaction temperature and reaction time). When immersion into the composite slurry, the surface of the PA matrix is chemically corroded and the polymer chains are loosened and then intertwine with that of the composite slurry. With the reaction going, the integration of the molecular chains between the substrate and the newly formed coating would be more sufficient at a higher temperature and longer reaction time. The molecular chains re-crystallize and wind together by hydrogen bonding after the phase change of ethanol from liquid to gas. Therefore, the bonding of coating to substrate is a kind of chemical bonding. Furthermore, higher shear strength can be obtained by adjusting the reaction conditions [8]. After interfacial bonding test, the pores of the fracture surface deform along the direction of the external load. Thus the graded porous coating can absorb energy more effectively by sufficient deformation and the gradient structure can uninterruptedly transfer the stress from the substrate to the coating layer. The corresponding EDS C and Ca-map scanning shows that C element is the main component of the fracture surface and no Ca element can be observed. This demonstrates that the fracture happens at the inner part of the corroded layer and the bonding strength inside the composite layer is strong enough to resist the shear force from the external load.

To construct the latter interface between the coating and bone tissues, nHA-rich coatings have been used to modify the surface of implants. The coating gives the implant properties that are quite different from the uncoated device and enables the implant to present a surface to the surrounding bone or soft tissue which elicits the optimum cell/tissue response [22]. In this study, cell response demonstrates that nHA/PA composite-coated samples contributed more to enhance the activity of osteoblast-like cells than the pure PA samples due to the support of nHA particles. From the results, it is obvious that the composite coating has a considerable influence on cell adhesion, spread and proliferation.

The results of *in vitro* experiments prompted us to study the composite-coated implants *in vivo*, so a rabbit model was used to investigate bone tissue response to composite-coated and uncoated implants. The interfacial strength between bone and implant biomaterials, as determined from push-out tests, is much greater for the bioactive coating implant compared with pure PA implant. The value of 3.49 ± 0.42 MPa found for composite-coated implants after 12 weeks implantation was on average 2.4 times higher than for the pure PA implants. The push-out tests have indicated that nHA-rich layer coatings enhance fixation of the implant in the surrounding bone.

In hard tissue replacement, the implants must interface with bone. The biocompatibility of implant materials is optimal when the material elicits the formation of normal tissues at its surface and establishes a contiguous interface capable of transferring the loads which normally occur at the implantation site. To what extent bone-plus-implant will be able to function as an integrated mechanical unit depends on the chemical, mechanical and physical properties of implant, and the interaction between bone and implant [22]. In this study, the construction of the composite coating gives the implant an entirely new surface with bioactive gradient properties. SEM shows intimate contact between the bone and the bioactive coated implant surface. EDS analyses show that the calcium and phosphorus concentration is not significantly different when scanning from the bone tissue to the interface, to the dense implant. Histological examination shows that the composite-coated PA implant becomes surrounded by fibrous tissue in the initial period of wound healing followed by osteoid deposition and bone formation. An integrated interface is created between the living bone tissue and the composite-coated implant.

5. Conclusion

The focus of this work is to combine the good mechanical properties of PA and the bioactivity of nHA. A chemical corrosion and phase inversion technique has been developed to fabricate a porous nHA gradient coating on a PA substrate. The nHA/PA composite coating exhibits a gradient variation in both microstructure and chemical composition. The shear strength of the composite coating with the PA substrate can reach 4.58 ± 0.14 MPa, and the fracture occurs inside the corrosion region. The cell response demonstrates that composite-coating samples have better cytocompatibility. Push-out test results illustrate that the shear strength of the composite-coated implants at 12 weeks post-implantation is remarkably stronger than the pure ones. According to the histological, SEM and EDS results, a compositionally graded and tissue-compatible interface is successfully achieved. This kind of coating design can significantly reduce the interfacial problems associated with the sharp interface present in conventional coating processing.

National guidelines for the care and use of laboratory animals were respected.

Funding statement. This work has been supported by the 863 National Key Project (no. 2011AA030102) and the Natural Science Foundation of China (no. 31370971), the support of the Scientific and Technological Innovation Programs of Higher Education Institutions in Shanxi (2013111), Natural Science Foundation of Shanxi Province (nos. 2013021014–2, 2013021003–1 and 2013021013–5), Program for the Outstanding Innovative Teams of Higher Learning Institutions of Shanxi (OIT), Program for the Young Teams of Taiyuan University of Technology (2013T066) and Taiyuan University of Technology Talents Fund is also acknowledged with gratitude.

References

1. Ma J, Liang CH, Kong LB, Wang C. 2003 Colloidal characterization and electrophoretic deposition of hydroxyapatite on titanium substrate. *J. Mater. Sci. Mater. Med.* **14**, 797–801. (doi:10.1023/a:1025092506583)
2. Roy M, Balla VK, Bandyopadhyay A, Bose S. 2011 Compositionally graded hydroxyapatite/tricalcium phosphate coating on Ti by laser and induction plasma. *Acta Biomater.* **7**, 866–873. (doi:10.1016/j.actbio.2010.09.016)
3. Carradó A. 2010 Structural, microstructural, and residual stress investigations of plasma-sprayed hydroxyapatite on Ti-6Al-4V. *ACS Appl. Mater. Interfaces* **2**, 561–565. (doi:10.1021/am900763j)
4. Kawai T, Ohtsuki C, Kamitakahara M, Miyazaki T, Tanihara M, Sakaguchi Y, Konagaya S. 2004 Coating of an apatite layer on polyamide films containing sulfonic groups by a biomimetic process. *Biomaterials* **25**, 4529–4534. (doi:10.1016/j.biomaterials.2003.11.039)
5. Kawai T, Ohtsuki C, Kamitakahara M, Hosoya K, Tanihara M, Miyazaki T, Sakaguchi Y, Konagaya S. 2007 *In vitro* apatite formation on polyamide containing carboxyl groups modified with silanol groups. *J. Mater. Sci. Mater. Med.* **18**, 1037–1042. (doi:10.1007/s10856-006-0081-2)
6. Cui W, Li X, Xie C, Zhuang H, Zhou S, Weng J. 2010 Hydroxyapatite nucleation and growth mechanism on electrospun fibers functionalized with different chemical groups and their combinations. *Biomaterials* **31**, 4620–4629. (doi:10.1016/j.biomaterials.2010.02.050)
7. Wong KL *et al*. 2009 Mechanical properties and *in vitro* response of strontium-containing hydroxyapatite/polyetheretherketone composites. *Biomaterials* **30**, 3810–3817. (doi:10.1016/j.biomaterials.2009.04.016)
8. Huang D, Zuo Y, Li J, Zou Q, Zhang L, Gong M, Wang L, Li L, Li Y. 2012 Bioactive composite gradient coatings of nano-hydroxyapatite/polyamide66 fabricated on polyamide66 substrates. *J. R. Soc. Interface* **9**, 1450–1457. (doi:10.1098/rsif.2011.0782)
9. Wang L, Li Y, Zuo Y, Zhang L, Zou Q, Cheng L, Jiang H. 2009 Porous bioactive scaffold of aliphatic polyurethane and hydroxyapatite for tissue regeneration. *Biomed. Mater.* **4**, 025003. (doi:10.1088/1748-6041/4/2/025003)
10. Su B, Peng X, Jiang D, Wu J, Qiao B, Li W, Qi X. 2013 *In vitro* and *in vivo* evaluations of nano-hydroxyapatite/polyamide 66/glass fibre (n-HA/PA66/GF) as a novel bioactive bone screw. *PLoS ONE* **8**, e68342. (doi:10.1371/journal.pone.0068342)
11. Wang H, Zuo Y, Zou Q, Cheng L, Huang D, Wang L, Li Y. 2009 Nano-hydroxyapatite/polyamide66 composite tissue-engineering scaffolds with anisotropy in morphology and mechanical behaviors. *J. Polym. Sci. A Polym. Chem.* **47**, 658–669. (doi:10.1002/pola.23171)
12. Olszta MJ, Cheng X, Jee SS, Kumar R, Kim YY, Kaufman MJ, Douglas EP, Gower LB. 2007 Bone structure and formation: a new perspective. *Mater. Sci. Eng. R* **58**, 77–116. (doi:10.1016/j.mser.2007.05.001)
13. Wang H, Li Y, Zuo Y, Li J, Ma S, Cheng L. 2007 Biocompatibility and osteogenesis of biomimetic nano-hydroxyapatite/polyamide composite scaffolds for bone tissue engineering. *Biomaterials* **28**, 3338–3348. (doi:10.1016/j.biomaterials.2007.04.014)
14. Shen J, Li Y, Zuo Y, Zou Q, Li J, Huang D, Wang X. 2009 Characterization and cytocompatibility of surface modified polyamide66. *J. Biomed. Mater. Res. B Appl. Biomater.* **91B**, 897–904. (doi:10.1002/jbm.b.31472)
15. Huang D, Zuo Y, Zou Q, Wang Y, Gao S, Wang X, Liu H, Li Y. 2012 Reinforced nanohydroxyapatite/polyamide66 scaffolds by chitosan coating for bone tissue engineering. *J. Biomed. Mater. Res. B Appl. Biomater.* **100B**, 51–57. (doi:10.1002/jbm.b.31921)
16. Glimcher MJ. 2006 Bone: nature of the calcium phosphate crystals and cellular, structural, and physical chemical mechanisms in their formation. *Rev. Mineral. Geochem.* **64**, 223–282. (doi:10.2138/rmg.2006.64.8)
17. Bonfield W, Grynpas MD, Tully AE, Bowman J, Abram J. 1981 Hydroxyapatite reinforced polyethylene: a mechanically compatible implant material for bone replacement. *Biomaterials* **2**, 185–186. (doi:10.1016/0142-9612(81)90050-8)
18. Gloria A, De Santis R, Ambrosio L, Causa F, Tanner KE. 2011 A multi-component fiber-reinforced PHEMA-based hydrogel/HAPEX device for customized intervertebral disc prosthesis. *J. Biomater. Appl.* **25**, 795–810. (doi:10.1177/0885328209360933)
19. Kim HW, Koh YH, Li LH, Lee S, Kim HE. 2004 Hydroxyapatite coating on titanium substrate with titania buffer layer processed by sol-gel method. *Biomaterials* **25**, 2533–2538. (doi:10.1016/j.biomaterials.2003.09.041)
20. Ohtsuki C, Kamitakahara M, Miyazaki T. 2007 Coating bone-like apatite onto organic substrates using solutions mimicking body fluid. *J. Tissue Eng. Regen. Med.* **1**, 33–38. (doi:10.1002/term.3)
21. Brohede U, Zhao S, Lindberg F, Mihranyan A, Forsgren J, Strømme M, Engqvist H. 2009 A novel graded bioactive high adhesion implant coating. *Appl. Surf. Sci.* **255**, 7723–7728. (doi:10.1016/j.apsusc.2009.04.149)
22. Paital SR, Dahotre NB. 2009 Calcium phosphate coatings for bio-implant applications: materials, performance factors, and methodologies. *Mater. Sci. Eng. R Rep.* **66**, 1–70. (doi:10.1016/j.mser.2009.05.001)
23. Yang S, Man HC, Xing W, Zheng X. 2009 Adhesion strength of plasma-sprayed hydroxyapatite coatings on laser gas-nitrided pure titanium. *Surf. Coat. Technol.* **203**, 3116–3122. (doi:10.1016/j.surfcoat.2009.03.034)
24. Yang YC, Chou BY. 2007 Bonding strength investigation of plasma-sprayed HA coatings on alumina substrate with porcelain intermediate layer. *Mater. Chem. Phys.* **104**, 312–319. (doi:10.1016/j.tsf.2009.03.122)
25. Sato K, Kogure T, Kumagai Y, Tanaka J. 2001 Crystal orientation of hydroxyapatite induced by ordered carboxyl groups. *J. Colloid Interface Sci.* **240**, 133–138. (doi:10.1006/jcis.2001.7617)
26. Song L, Gan L, Xiao YF, Wu Y, Wu F, Gu ZW. 2011 Antibacterial hydroxyapatite/chitosan complex coatings with superior osteoblastic cell response. *Mater. Lett.* **65**, 974–977. (doi:10.1016/j.matlet.2010.12.051)
27. Negroiu G, Piticescu R, Chitanu G, Mihailescu I, Zdrentu L, Miroiu M. 2008 Biocompatibility evaluation of a novel hydroxyapatite–polymer coating for medical implants (*in vitro* tests). *J. Mater. Sci. Mater. Med.* **19**, 1537–1544. (doi:10.1007/s10856-007-3300-6)
28. Muthutantri A, Huang J, Edirisinghe M. 2008 Novel preparation of graded porous structures for medical engineering. *J. R. Soc. Interface* **5**, 1459–1467. (doi:10.1098/rsif.2008.0092)
29. Zhang X, Li YB, Zuo Y, Lv GY, Mu YH, Li H. 2007 Morphology, hydrogen-bonding and crystallinity of nano-hydroxyapatite/polyamide 66 biocomposites. *Compos. A Appl. Sci. Manuf.* **38**, 843–848. (doi:10.1016/j.compositesa.2006.08.002)
30. Li YB, de Wijn J, Klein CPAT, van der Meer S, de Groot K. 1994 Preparation and characterization of nanograde osteoapatite-like rod crystals. *J. Mater. Sci. Mater. Med.* **5**, 252–255. (doi:10.1007/bf00122393)

31. Zhang E, Zou C, Zeng S. 2009 Preparation and characterization of silicon-substituted hydroxyapatite coating by a biomimetic process on titanium substrate. *Surf. Coat. Technol.* **203**, 1075–1080. (doi:10.1016/j.surfcoat.2008.09.038)
32. Link DP, van den Dolder J, Jurgens WJFM, Wolke JGC, Jansen JA. 2006 Mechanical evaluation of implanted calcium phosphate cement incorporated with PLGA microparticles. *Biomaterials* **27**, 4941–4947. (doi:10.1016/j.biomaterials.2006.05.022)
33. Surmenev RA, Surmeneva MA, Ivanova AA. 2014 Significance of calcium phosphate coatings for the enhancement of new bone osteogenesis: a review. *Acta Biomater.* **10**, 557–579. (doi:10.1016/j.actbio.2013.10.036)
34. Tayton E *et al*. 2013 A comparison of polymer and polymer–hydroxyapatite composite tissue engineered scaffolds for use in bone regeneration. An *in vitro* and *in vivo* study. *J. Biomed. Mater. Res. A* **102**, 2613–2624. (doi:10.1002/jbm.a.34926)
35. Kim MS, Khang G, Lee HB. 2008 Gradient polymer surfaces for biomedical applications. *Progress Polym. Sci.* **33**, 138–164. (doi:10.1016/j.progpolymsci.2007.06.001)
36. Tanahashi M, Yao T, Kokubo T, Minaoda M, Miyamoto T, Nakamura T, Yamamuro T. 1995 Apatite coated on organic polymers by biomimetic process: improvement in adhesion to substrate by HCl treatment. *J. Mater. Sci. Mater. Med.* **6**, 319–326. (doi:10.1007/BF00120299)